NASA TECHNICAL NOTE

NASA TN D-6955

NASA TN D-6955

AN ELASTIC ANALYSIS OF STRESSES IN A UNIAXIALLY LOADED SHEET CONTAINING AN INTERFERENCE-FIT BOLT

by John H. Crews, Jr.

Langley Research Center
Hampton, Va. 23365

NATIONAL AERONAUTICS AND SPACE ADMINISTRATION • WASHINGTON, D. C. • OCTOBER 1972

1. Report No.	2. Government Accession No.	3. Recipient's Catalog No.
NASA TN D-6955		

4. Title and Subtitle	5. Report Date
AN ELASTIC ANALYSIS OF STRESSES IN A UNIAXIALLY LOADED SHEET CONTAINING AN INTERFERENCE-FIT BOLT	October 1972
	6. Performing Organization Code

7. Author(s)	8. Performing Organization Report No.
John H. Crews, Jr.	L-8415
	10. Work Unit No. 501-22-02-01
9. Performing Organization Name and Address	11. Contract or Grant No.
NASA Langley Research Center Hampton, Va. 23365	
	13. Type of Report and Period Covered
12. Sponsoring Agency Name and Address	Technical Note
National Aeronautics and Space Administration Washington, D.C. 20546	14. Sponsoring Agency Code

15. Supplementary Notes

16. Abstract

The stresses in a sheet with an interference-fit bolt have been calculated for two sheet-bolt interface conditions: a frictionless interface and a fixed (no-slip) interface. The stress distributions were calculated for various combinations of sheet and bolt moduli. The results show that for repeated loading the local stress range is significantly smaller if an interference bolt is used instead of a loosely fitting one. This reduction in local stress range is more pronounced when the ratio of bolt modulus to sheet modulus is large. The analysis also indicates that currently used standard values of interference cause yielding in the sheet.

17. Key Words (Suggested by Author(s))	18. Distribution Statement
Elastic sheet Interference-fit bolt Stress analysis Bolt-sheet separation Sheet yielding	Unclassified – Unlimited

19. Security Classif. (of this report)	20. Security Classif. (of this page)	21. No. of Pages	22. Price*
Unclassified	Unclassified	27	$3.00

*For sale by the National Technical Information Service, Springfield, Virginia 22151

AN ELASTIC ANALYSIS OF STRESSES IN A UNIAXIALLY LOADED SHEET CONTAINING AN INTERFERENCE-FIT BOLT

By John H. Crews, Jr.
Langley Research Center

SUMMARY

The stresses in a sheet with an interference-fit bolt have been calculated for two sheet-bolt interface conditions: a frictionless interface and a fixed (no-slip) interface. The stress distributions were calculated for various combinations of sheet and bolt moduli. The results show that for repeated loading the local stress range is significantly smaller if an interference bolt is used instead of a loosely fitting one. This reduction in local stress range is more pronounced when the ratio of bolt modulus to sheet modulus is large. The analysis also indicates that currently used standard values of interference cause yielding in the sheet.

INTRODUCTION

Laboratory studies have shown that structural joints with interference-fit bolts have longer fatigue lives than those with loosely fitted bolts (ref. 1). As a result, interference-fit bolts are used in aircraft structures (refs. 2 and 3), although the underlying phenomenon which lengthens life is not completely understood. An analysis of the phenomenon was presented in reference 4, but unfortunately, the solution does not provide a clear explanation of the phenomenon nor does it lend itself to a systematic analysis of the problem. The purpose of the present report is to present a more complete elastic analysis of stresses in a sheet containing an interference-fit bolt and to discuss the influence of interference fits on fatigue life.

The analysis is based on a general solution presented in references 5 and 6 for a uniaxially loaded infinite sheet with a circular hole containing an elastic disk insert. Two special solutions were examined – the first was for a frictionless interface between the sheet and bolt; the second was for a no-slip interface. These two idealizations bracket the real interface behavior, which is expected to involve some slip.

Results are presented in terms of applied stress, interference, and material constants for the sheet and bolt. Stress distributions are presented for typical combinations

of sheet and bolt materials and are used to explain the effects of interference bolts on fatigue life. Applicable ranges for the solution are presented in terms of the combinations of applied stress and interference that produce either yielding of the sheet or separation at the sheet-bolt interface.

SYMBOLS

The units used for the physical quantities defined in this paper are given in the International System of Units (SI) (ref. 7) and in the U.S. Customary Units. The measurements and calculations were made in the U.S. Customary Units.

a_1, a_2, a_3 unknown coefficients in complex stress functions for a sheet with a circular hole

b_1, b_2, b_3 unknown coefficients in complex stress functions for a disk

D diameter of hole, mm (in.)

E Young's modulus, MN/m^2 (ksi)

I interference, or difference between bolt and hole diameters, mm (in.)

R radial distance to bolt-sheet interface, mm (in.)

r, θ polar coordinates, mm (in.) and deg

S nominal stress, MN/m^2 (ksi)

v_r, v_θ displacements, mm (in.)

x,y Cartesian coordinates, mm (in.)

z complex variable, $x + iy$

ν Poisson's ratio

$\sigma_{rr}, \sigma_{\theta\theta}$ normal stress components, MN/m^2 (ksi)

$\bar{\sigma}_{rr}, \bar{\sigma}_{\theta\theta}$ normal stress components caused by interference fit between bolt and sheet, MN/m^2 (ksi)

σ_y yield stress, MN/m^2 (ksi)

$\tau_{r\theta}$ shear stress component, MN/m^2 (ksi)

ϕ, ψ complex stress functions

Subscripts:

1 denotes sheet

2 denotes bolt

s separation

ANALYSIS

Figure 1 shows the problem analyzed in this study. The sheet was assumed to be infinite and the interference-fit bolt was represented by a disk equal in thickness to that of the sheet. The analysis was further simplified by assuming a state of plane elastic stress for both the sheet and bolt. This analysis becomes invalid when the hole deforms so much that the sheet separates from the bolt.

The solution for this problem was taken from references 5 and 6 and is briefly described in the appendix. The stress equations for the sheet are as follows (see eqs. (A3) to (A5)):

$$\left.\begin{aligned}
\sigma_{rr_1}(r,\theta) &= \frac{S}{2}\left\{1 - \frac{a_2}{2}\left(\frac{R}{r}\right)^2 - \left[1 + 2a_1\left(\frac{R}{r}\right)^2 + \frac{3}{2}a_3\left(\frac{R}{r}\right)^4\right]\cos 2\theta\right\} \\
\sigma_{\theta\theta_1}(r,\theta) &= \frac{S}{2}\left\{1 + \frac{a_2}{2}\left(\frac{R}{r}\right)^2 + \left[1 + \frac{3}{2}a_3\left(\frac{R}{r}\right)^4\right]\cos 2\theta\right\}
\end{aligned}\right\} \qquad (1)$$

and

$$\tau_{r\theta_1}(r,\theta) = \frac{S}{2}\left[1 - a_1\left(\frac{R}{r}\right)^2 - \frac{3}{2}a_3\left(\frac{R}{r}\right)^4\right]\sin 2\theta$$

The undetermined coefficients a_i were evaluated for both the frictionless and no-slip cases by specifying stress and displacement conditions at the sheet-bolt interface, as explained in the appendix.

Because the analysis was based on the assumption of elastic material response, local yielding of the sheet material represents a limiting condition for the solutions. Yielding can be caused by high interference stresses alone or by the combined effect of interference stresses and stresses produced by remote loading of the sheet. Yielding was assumed to be governed by the Mises yield condition:

$$\sigma_y = \left(\sigma^2_{rr_1} - \sigma_{rr_1}\sigma_{\theta\theta_1} + \sigma^2_{\theta\theta_1} + 3\tau^2_{r\theta_1}\right)^{1/2} \tag{2}$$

Yielding is usually expected to initiate at the points of maximum stress concentration which lie on the interface boundary at the x-axis; however, for the no-slip case the interface shear stresses reach a maximum away from this axis and therefore can change the location for initial yielding. This possibility was examined by evaluating equation (2) at 5^o intervals along the interface. The desired limits for the solution were expressed in terms of interference and applied stress levels which cause yielding for various ratios of Young's moduli E_2/E_1.

In addition to the assumption of elastic material behavior, the sheet was assumed to be in contact with the bolt along the entire interface. Loading of the sheet eventually causes separation at the intersection of the y-axis and the interface. Since separation corresponds to zero-load transfer at these two points, a condition for the onset of separation was established by setting $\sigma_{rr_1}\left(R, \frac{\pi}{2}\right)$ equal to zero. The result was an equation for the stress S_S, which when applied to the sheet corresponds to incipient separation at the interface.

For the frictionless case, the separation stress was found from equation (A18) to be

$$S_S = \frac{IE_1}{2R}\left[\frac{3 + \nu_2 + (5 - \nu_1)\frac{E_2}{E_1}}{9 - 5\nu_2 + (11 + 5\nu_1)\frac{E_2}{E_1}}\right] \tag{3}$$

where I is interference, E is Young's modulus, ν is Poisson's ratio, and the subscripts 1 and 2 denote the sheet and bolt, respectively. For the no-slip case, equation (A25) gave

$$S_S = \frac{IE_1}{2R}\left[\frac{1 + \nu_2 + (3 - \nu_1)\frac{E_2}{E_1}}{3 - \nu_2 + (5 + \nu_1)\frac{E_2}{E_1}}\right] \tag{4}$$

RESULTS AND DISCUSSION

Because fatigue failures usually occur in the sheet rather than the bolt, only stresses in the sheet will be discussed. Stresses for a sheet with an interference-fit bolt are compared with those for a sheet with an open hole. For comparison, stresses for the open-hole case are presented in figure 2, where the local stresses have been normalized by the applied stress S. As expected, the normalized stress peaked at $\sigma_{\theta\theta} = 3$ at $\theta = 0$. The familiar distributions of $\sigma_{\theta\theta}$ and σ_{rr} along the transverse axis of symmetry are shown in figure 2(b). Since only stresses for the sheet are presented, the subscript 1 has been dropped.

Frictionless Interface

Stresses in figure 3 are for sheet and bolt materials with identical moduli. For convenience, the stresses are normalized by S_s, the applied stress for incipient separation at the interface. The interference stresses, produced solely by the interference fit, are indicated by $\bar{\sigma}_{rr}$ and $\bar{\sigma}_{\theta\theta}$ and are represented by dashed lines; these stresses are uniform along the boundary of the hole (fig. 3(a)) and, as expected, approach zero away from the hole (fig. 3(b)). The combined effect of interference and the applied stress is shown by the solid curves. If the applied stress is cycled between 0 and S_s, the stresses in the sheet cycle between the dashed and solid curves. Comparison of these curves in figure 3(a) shows that the maximum local stress range is only 1.75 (1.25 to 3.0), which is considerably smaller than the range 3.0 for the case of a loosely fitting bolt. This smaller local stress range is responsible for the improvement in fatigue life attributable to interference-fit fasteners. It should be noted that this smaller local stress range is accompanied by a larger local mean stress which tends to reduce the benefit of the interference fit on fatigue life.

The stresses in figure 4 for $\frac{E_2}{E_1} = 3$ represent elastic behavior typical of an aluminum sheet with a steel bolt. The maximum value of $\sigma_{\theta\theta}$ again equals 3.0, but since $\bar{\sigma}_{\theta\theta} = 1.67$ for this case, the maximum local stress range is only 1.33, compared with 1.75 for $\frac{E_2}{E_1} = 1$, and 3.0 for the loose bolt. Thus, the local stress range is smaller for larger values of E_2/E_1. This effect is illustrated in figure 5. As E_2/E_1 increases from zero, the local stress range decreases rapidly and approaches the limiting value of about 0.95 for $\frac{E_2}{E_1} = \infty$ (rigid bolt). For cyclic loading from 0 to S_s, $\sigma_{\theta\theta}$ cycles between values given by the dashed and solid curves.

Limits for the frictionless-fit solution are presented in figure 6 in terms of curves corresponding to separation of the sheet-bolt interface and yielding of the sheet. The

separation curves, calculated from equation (3), show only a minor dependence on E_2/E_1. In contrast, the yield curves, equation (2), are strongly dependent on E_2/E_1. For a given E_2/E_1 value, the range of validity for the present solution is represented by the region under a corresponding pair of separation and yielding curves. In all frictionless-fit cases, yielding started at the intersection of the x-axis and the interface.

Note that the intersection of the yield curves and the I/D axis represent yielding due to interference alone. For the typical values of $\frac{E_2}{E_1} = 1$ and 3, yielding occurs for $\frac{I}{D} = 0.0081$ and 0.0062, respectively. Since standard values of I/D for interference bolts currently in use range from 0.007 to 0.017 (for D = 6.35 mm (0.25 in.), ref. 8), yielding due to interference-bolt installation is common. The less widely used "low interference" bolts (ref. 8) have I/D values of 0.0008 to 0.0060, which lie within the range of the present elastic solution.

No-Slip Interface

Stresses in a sheet with a no-slip interference bolt are shown in figure 7 for $\frac{E_2}{E_1} = 1$. The interference stresses for this case appear smaller than those for the corresponding frictionless case $\left(\bar{\sigma}_{\theta\theta} = 1.0 \text{ compared with } 1.25 \text{ from fig. } 3\right)$ because the value of S_s used to normalize $\bar{\sigma}_{\theta\theta}$ is larger for the no-slip case. This larger value of S_s can be attributed to the shear stresses that develop at the no-slip interface when the sheet is loaded (fig. 7(a)). These stresses cause larger load transfer across the interface and therefore less load transfer around the bolt hole. Consequently, the strains (displacements) in the sheet that contribute to separation are smaller and thus permit larger values of S_s.

When stress is applied to the sheet, the maximum value of $\sigma_{\theta\theta}$ increases from 1.0 to 2.0 – a local stress range of 1.0. Since $\frac{E_2}{E_1} = 1$, and both shear and normal stresses are transferred across the interface, the hole is in effect eliminated by the presence of the bolt. Therefore, a local stress range equal to the applied stress range is expected. This is illustrated in figure 7(b), where the $\sigma_{\theta\theta}$ curve is identical with the $\bar{\sigma}_{\theta\theta}$ curve when it is displaced vertically by 1.0.

Stresses for $\frac{E_2}{E_1} = 3$ are presented in figure 8. Although the interference stress at the interface is larger than that for the previous case $\left(\frac{E_2}{E_1} = 1\right)$, the maximum local stress increases by only 0.45 to a value of 1.73 when the sheet is loaded. Thus, for $\frac{E_2}{E_1} = 3$, a

no-slip interference fit is very effective in reducing the local cyclic stress range (0.45 compared with 3.0 for the loosely fitting bolt). In fact, the local stress range at the bolt hole is smaller than that away from the hole, as shown in figure 8(b).

The general influence of E_2/E_1 on local stress range for the no-slip case is shown in figure 9. Local stress range decreases abruptly as E_2/E_1 increases from zero, and it approaches zero for the rigid-bolt case $\left(\frac{E_2}{E_1} = \infty\right)$. Note that for the loading used (0 to S_S), the local mean stress is independent of E_2/E_1. Therefore, the decrease in local stress range is achieved without the accompanying increase in local mean stress observed for the frictionless-fit case.

Limits for the no-slip interference fit solution are shown in figure 10. These are similar to the curves for the frictionless fit in figure 6, but comparison shows that the range of applicability for the no-slip case is somewhat larger; that is, higher stresses can be applied without causing either separation or yielding. The point of initial yielding at the interface is shifted away from the x-axis by the shear stresses that develop along the interface when the sheet is loaded. For $\frac{E_2}{E_1} = 1$ and 3, this shift is less than 5°; but for $\frac{E_2}{E_1} = \infty$, initial yielding occurs at about $\theta = 25^\circ$.

CONCLUDING REMARKS

The stresses in a uniaxially loaded sheet containing an interference-fit bolt have been calculated. These calculations explain why interference bolts lengthen fatigue life of aircraft structural components. Two special cases were examined – the first was based on a frictionless interface between the sheet and bolt; the second was based on a no-slip interface. These two idealizations bracket the real behavior at the interface, which is expected to involve some slip between the sheet and bolt.

Both solutions show that for cyclic loading the range of local stresses at the bolt hole can be reduced significantly by using an interference-fit bolt instead of a loosely fitting bolt. The reduction is larger for the no-slip case and is more pronounced when a high-modulus bolt is used in a low-modulus sheet.

For the frictionless case, the local stresses caused by interference and those caused by an applied stress S_S, corresponding to incipient separation at the interface, combine to produce a maximum circumferential stress at the bolt hole equal to three times the applied stress. This is identical with the stress at a hole with a loosely fitting bolt. Therefore, the reduction in local stress range is due solely to the largely minimum local stress caused by the interference fit.

For the no-slip case, the maximum local stress is smaller than that for an open hole. The reduction in local stress range results from a smaller maximum local stress combined with a larger minimum stress due to interference. For cyclic loading from 0 to S_S, the local mean stress for this case is equal to that for the case of a loosely fitting bolt.

An analysis of the stresses due solely to interference reveals that the standard values of interference currently in use usually cause sheet yielding during bolt installation. Therefore, elastoplastic methods are required for a complete analysis of structural members containing interference-fit bolts.

Langley Research Center,
National Aeronautics and Space Administration,
Hampton, Va., September 12, 1972.

APPENDIX

STRESS AND DISPLACEMENT EQUATIONS

The desired stress and displacement equations for the problem of an interference-fit bolt in an infinite sheet under uniaxial load can be obtained from either reference 5 or 6. In reference 5, Muskhelishvili presented a solution for an unloaded infinite sheet with an interference-fit disk and a solution for a uniaxially loaded sheet with a noninterference disk as an insert. If the disk is assumed to represent a bolt, the desired equations may be obtained by superposition of these two solutions. In reference 6, Savin presented a solution for a uniaxially loaded sheet with a hole reinforced by rings. He specialized this solution for the case of a single ring, then introduced interference, and finally set the inner radius of the ring equal to zero to represent an interference-fit disk. For this specialized case, the Savin solution reduces to that obtainable by superimposing the two Muskhelishvili solutions.

The following development, although mathematically equivalent to the Muskhelishvili and Savin solutions, is presented in a more direct and complete manner.

General Stress and Displacement Equations

The stress and displacement equations were developed by the complex-variable approach (see, e.g., ref. 5). Accordingly, stresses σ_{rr}, $\sigma_{\theta\theta}$, and $\tau_{r\theta}$ and the displacements v_r and v_θ were expressed in terms of complex stress functions $\phi(z)$ and $\psi(z)$. For the case of plane stress,

$$\left.\begin{aligned}
\sigma_{rr} + \sigma_{\theta\theta} &= 2\left[\phi'(z) + \overline{\phi'(z)}\right] \\
\sigma_{\theta\theta} - \sigma_{rr} + 2i\tau_{r\theta} &= 2\left[\bar{z}\phi''(z) + \psi'(z)\right]e^{2i\theta} \\
\frac{E}{1+\nu}\left(v_r + iv_\theta\right) &= \left[\frac{3-\nu}{1+\nu}\phi(z) - z\overline{\phi'(z)} - \overline{\psi(z)}\right]e^{-i\theta}
\end{aligned}\right\} \tag{A1}$$

The stress functions $\phi_1(z)$ and $\psi_1(z)$ for the sheet were taken from reference 5. After a slight modification to change the loading from the x-direction to the y-direction, as shown in figure 1, they were expressed as

$$\phi_1(z) = \frac{SR_1}{4}\left(\frac{z}{R_1} + a_1\frac{R_1}{z}\right) \tag{A2a}$$

and

$$\psi_1(z) = -\frac{SR_1}{4}\left(-2\frac{z}{R_1} + a_2\frac{R_1}{z} + a_3\frac{R_1^3}{z^3}\right) \tag{A2b}$$

where R_1 is the radius of the hole and a_1, a_2, and a_3 are unknown coefficients. The functions $\phi_1(z)$ and $\psi_1(z)$ were substituted in equations (A1) which were then solved for stresses and displacements; in terms of polar coordinates these equations were expressed as

$$\sigma_{rr_1}(r,\theta) = \frac{S}{2}\left\{1 - \frac{a_2}{2}\left(\frac{R_1}{r}\right)^2 - \left[1 + 2a_1\left(\frac{R_1}{r}\right)^2 + \frac{3}{2}a_3\left(\frac{R_1}{r}\right)^4\right]\cos 2\theta\right\} \tag{A3}$$

$$\sigma_{\theta\theta_1}(r,\theta) = \frac{S}{2}\left\{1 + \frac{a_2}{2}\left(\frac{R_1}{r}\right)^2 + \left[1 + \frac{3}{2}a_3\left(\frac{R_1}{r}\right)^4\right]\cos 2\theta\right\} \tag{A4}$$

$$\tau_{r\theta_1}(r,\theta) = \frac{S}{2}\left[1 - a_1\left(\frac{R_1}{r}\right)^2 - \frac{3}{2}a_3\left(\frac{R_1}{r}\right)^4\right]\sin 2\theta \tag{A5}$$

$$v_{r_1}(r,\theta) = \frac{SR_1(1+\nu_1)}{4E_1}\left\{\frac{2(1-\nu_1)}{1+\nu_1}\frac{r}{R_1} + \frac{a_2R_1}{r} + \left[-\frac{2r}{R_1} + \frac{4a_1R_1}{r(1+\nu_1)} + a_3\left(\frac{R_1}{r}\right)^3\right]\cos 2\theta\right\} \tag{A6}$$

and

$$v_{\theta_1}(r,\theta) = \frac{SR_1(1+\nu_1)}{4E_1}\left[\frac{2r}{R_1} - 2a_1\frac{1-\nu_1}{1+\nu_1}\frac{R_1}{r} + a_3\left(\frac{R_1}{r}\right)^3\right]\sin 2\theta \tag{A7}$$

The stress functions for the bolt were (ref. 5)

$$\left.\begin{aligned}\phi_2(z) &= \frac{SR_2}{4}\left[b_1\left(\frac{z}{R_2}\right)^3 + \frac{b_2z}{R_2}\right] \\ \text{and} \\ \psi_2(z) &= -\frac{SR_2}{4}\left(\frac{b_3z}{R_2}\right)\end{aligned}\right\} \tag{A8}$$

where R_2 is the bolt radius and b_i are unknown coefficients. Substitution of $\phi_2(z)$ and $\psi_2(z)$ into equations (A1) yields

$$\sigma_{rr_2}(r,\theta) = \frac{S}{2}\left(b_2 + \frac{b_3}{2}\cos 2\theta\right) \tag{A9}$$

$$\sigma_{\theta\theta_2}(r,\theta) = \frac{S}{2}\left\{b_2 - \left[\frac{b_3}{2} - 6b_1\left(\frac{r}{R_2}\right)^2\right]\cos 2\theta\right\} \tag{A10}$$

$$\tau_{r\theta_2}(r,\theta) = \frac{3}{2}\left[3b_1\left(\frac{r}{R_2}\right)^2 - \frac{b_3}{2}\right]\sin 2\theta \tag{A11}$$

$$v_{r_2}(r,\theta) = \frac{SR_2}{4E_2}\left\{2(1-\nu_2)\frac{b_2 r}{R_2} - \left[4\nu_2 b_1\left(\frac{r}{R_2}\right)^3 - (1+\nu_2)b_3\frac{r}{R_2}\right]\cos 2\theta\right\} \tag{A12}$$

and

$$v_{\theta_2}(r,\theta) = \frac{SR_2}{4E_2}\left[2(3+\nu_2)b_1\left(\frac{r}{R_2}\right)^3 - (1+\nu_2)b_3\frac{r}{R_2}\right]\sin 2\theta \tag{A13}$$

The general stress and displacement equations (A3) to (A7) and (A9) to (A13) were used in each of the two following solutions.

Frictionless Interface

An interference fit between a disk of radius R_2 and a hole of radius R_1 can be expressed as

$$R_2 - R_1 = \frac{I}{2} > 0$$

where I is the interference. After the disk has been inserted into the hole, the disk-sheet interface lies at radius R, where $R_1 < R < R_2$. For simplicity, R_1 and R_2 are replaced by R in the stress and displacement equations; since I is much smaller than R_1 and R_2, only small errors (less than 1 percent) are introduced.

For the case of an interference fit with a frictionless interface, the following conditions must be satisfied on the interface:

$$\sigma_{rr_1}(R,\theta) = \sigma_{rr_2}(R,\theta) \tag{A14}$$

$$\tau_{r\theta_1}(R,\theta) = 0 \tag{A15}$$

$$\tau_{r\theta_2}(R,\theta) = 0 \tag{A16}$$

$$v_{r_1}(R,\theta) - v_{r_2}(R,\theta) = \frac{I}{2} \tag{A17}$$

The appropriate stress and displacement expressions from the general solution were substituted into these interface equations. Two additional equations were obtained by separating algebraic and trigonometric terms in equations (A14) and (A16). The resulting set of six equations was solved for the six unknown coefficients in the general solution. The following coefficients were determined:

$$a_1 = -2 + \frac{12\,\frac{E_2}{E_1}}{3 + \nu_2 + \left(5 - \nu_1\right)\frac{E_2}{E_1}}$$

$$a_2 = 2 - \frac{4\left(1 - \frac{IE_1}{2SR}\right)\frac{E_2}{E_1}}{1 - \nu_2 + \left(1 + \nu_1\right)\frac{E_2}{E_1}}$$

$$a_3 = 2 - \frac{8\,\frac{E_2}{E_1}}{3 + \nu_2 + \left(5 - \nu_1\right)\frac{E_2}{E_1}}$$

$$b_1 = \frac{-4\,\frac{E_2}{E_1}}{3 + \nu_2 + \left(5 - \nu_1\right)\frac{E_2}{E_1}}$$

$$b_2 = \frac{2\left(1 - \frac{IE_1}{2SR}\right)\frac{E_2}{E_1}}{1 - \nu_2 + \left(1 + \nu_1\right)\frac{E_2}{E_1}}$$

and

$$b_3 = \frac{-24\,\frac{E_2}{E_1}}{3 + \nu_2 + \left(5 - \nu_1\right)\frac{E_2}{E_1}}$$

These coefficients were substituted into equations (A3) to (A5) to find the following equations for stresses in the sheet:

$$\sigma_{rr_1} = \frac{S}{2}\left(1 - \left[1 - \frac{\left(2 - \frac{IE_1}{SR}\right)\frac{E_2}{E_1}}{1 - \nu_2 + \left(1 + \nu_1\right)\frac{E_2}{E_1}}\right]\left(\frac{R}{r}\right)^2 - \left\{1 + 4\left[-1 + \frac{6\,\frac{E_2}{E_1}}{3 + \nu_2 + \left(5 - \nu_1\right)\frac{E_2}{E_1}}\right]\left(\frac{R}{r}\right)^2 + 3\left[1 - \frac{4\,\frac{E_2}{E_1}}{3 + \nu_2 + \left(5 - \nu_1\right)\frac{E_2}{E_1}}\right]\left(\frac{R}{r}\right)^4\right\}\cos 2\theta\right) \tag{A18}$$

$$\sigma_{\theta\theta_1} = \frac{S}{2}\left(1 + \left[1 - \frac{\left(2 - \frac{IE_1}{SR}\right)\frac{E_2}{E_1}}{1 - \nu_2 + \left(1 + \nu_1\right)\frac{E_2}{E_1}}\right]\left(\frac{R}{r}\right)^2 + \left\{1 + 3\left[1 - \frac{4\,\frac{E_2}{E_1}}{3 + \nu_2 + \left(5 - \nu_1\right)\frac{E_2}{E_1}}\right]\left(\frac{R}{r}\right)^4\right\}\cos 2\theta\right) \tag{A19}$$

and

$$\tau_{r\theta_1} = \frac{S}{2}\left\{1 + 2\left[1 - \frac{6\,\frac{E_2}{E_1}}{3 + \nu_2 + \left(5 - \nu_1\right)\frac{E_2}{E_1}}\right]\left(\frac{R}{r}\right)^2 - 3\left[1 - \frac{4\,\frac{E_2}{E_1}}{3 + \nu_2 + \left(5 - \nu_1\right)\frac{E_2}{E_1}}\right]\left(\frac{R}{r}\right)^4\right\} \sin 2\theta \tag{A20}$$

No-Slip Interface

For the case of a no-slip interface the following interface conditions were used:

$$\sigma_{rr_1}(R,\theta) = \sigma_{rr_2}(R,\theta) \tag{A21}$$

$$\tau_{r\theta_1}(R,\theta) = \tau_{r\theta_2}(R,\theta) \tag{A22}$$

$$v_{r_1}(R,\theta) - v_{r_2}(R,\theta) = \frac{I}{2} \tag{A23}$$

$$v_{\theta_1}(R,\theta) = v_{\theta_2}(R,\theta) \tag{A24}$$

Two additional equations were obtained by separating algebraic and trigonometric terms in equations (A22) and (A24). The following coefficients were determined from the set of six equations:

$$a_1 = -2 + \frac{8\,\frac{E_2}{E_1}}{1 + \nu_2 + \left(3 - \nu_1\right)\frac{E_2}{E_1}}$$

$$a_2 = 2 - \frac{4\left(1 - \frac{IE_1}{2SR}\right)\frac{E_2}{E_1}}{1 - \nu_2 + (1 + \nu_1)\frac{E_2}{E_1}}$$

$$a_3 = 2 - \frac{8\,\frac{E_2}{E_1}}{1 + \nu_2 + (3 - \nu_1)\frac{E_2}{E_1}}$$

$$b_1 = 0$$

$$b_2 = \frac{2\left(1 - \frac{IE_1}{2SR}\right)\frac{E_2}{E_1}}{1 - \nu_2 + (1 + \nu_1)\frac{E_2}{E_1}}$$

and

$$b_3 = \frac{-8\,\frac{E_2}{E_1}}{1 + \nu_2 + (3 - \nu_1)\frac{E_2}{E_1}}$$

These coefficients were substituted into equations (A3) to (A5) to obtain the desired equations for stress in the sheet:

$$\sigma_{rr_1} = \frac{S}{2}\left(1 - \left[1 - \frac{\left(2 - \frac{IE_1}{SR}\right)\frac{E_2}{E_1}}{1 - \nu_2 + (1 + \nu_1)\frac{E_2}{E_1}}\right]\left(\frac{R}{r}\right)^2 - \left\{1 - \left[1 - \frac{4\,\frac{E_2}{E_1}}{1 + \nu_2 + (3 - \nu_1)\frac{E_2}{E_1}}\right]\left[4\left(\frac{R}{r}\right)^2 - 3\left(\frac{R}{r}\right)^4\right]\right\}\cos 2\theta\right) \qquad \text{(A25)}$$

$$\sigma_{\theta\theta_1} = \frac{S}{2}\left(1 + \left[1 - \frac{\left(2 - \frac{IE_1}{SR}\right)\frac{E_2}{E_1}}{1 - \nu_2 + (1 + \nu_1)\frac{E_2}{E_1}}\right]\left(\frac{R}{r}\right)^2 + \left\{1 + 3\left[1 - \frac{4\,\frac{E_2}{E_1}}{1 + \nu_2 + (3 - \nu_1)\frac{E_2}{E_1}}\right]\left(\frac{R}{r}\right)^4\right\}\cos 2\theta\right) \tag{A26}$$

$$\tau_{r\theta_1} = \frac{S}{2}\left\{1 + \left[1 - \frac{4\,\frac{E_2}{E_1}}{1 + \nu_2 + (3 - \nu_1)\frac{E_2}{E_1}}\right]\left[2\left(\frac{R}{r}\right)^2 - 3\left(\frac{R}{r}\right)^4\right]\right\}\sin 2\theta \tag{A27}$$

REFERENCES

1. Smith, Clarence R.: Interference Fasteners for Fatigue-Life Improvement. Exp. Mech., vol. 5, no. 8, Aug. 1965, pp. 19A-23A.

2. Smith, Clarence R.: Taper-Lok Bolts – Digest of Test Data and Users' Experiences. NAEC-ASL-1088, U.S. Navy, Mar. 1965.

3. Hinders, Urban A.: F-111 Design Experience – Use of High Strength Steel. AIAA Paper No. 70-884, July 1970.

4. Regalbuto, J. A.; and Wheeler, O. E.: Stress Distributions From Interference Fits and Uniaxial Tension. Exp. Mech., vol. 10, no. 7, July 1970, pp. 274-280.

5. Muskhelishvili, N. I. (J. R. M. Radok, transl.): Some Basic Problems of the Mathematical Theory of Elasticity. Fourth ed., P. Noordhoff, Ltd. (Groningen), 1963, pp. 216-223.

6. Savin, G. N. (Eugene Gros, transl.): Stress Concentration Around Holes. Pergamon Press, Inc., 1961, pp. 234-257.

7. Comm. on Metric Pract.: ASTM Metric Practice Guide. NBS Handbook 102, U.S. Dep. Com., Mar. 10, 1967.

8. Mead, Daniel R.: Taper-Lok Reference Manual. Second ed., Briles Manufacturing, c.1967.

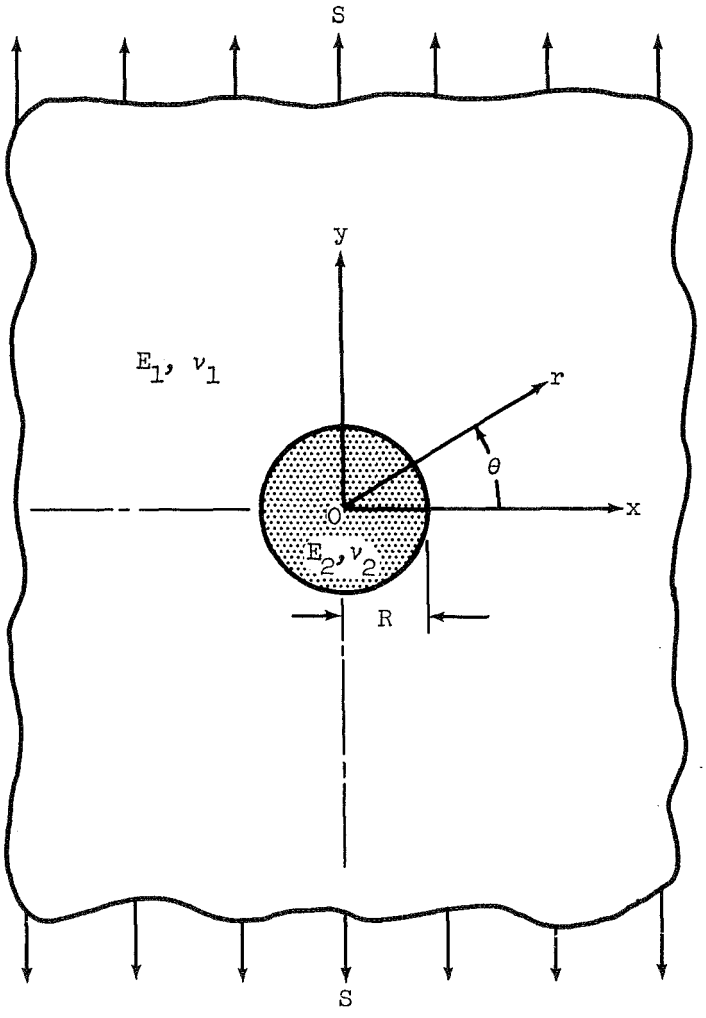

Figure 1.- Sheet under uniaxial stress with an interference-fit disk.

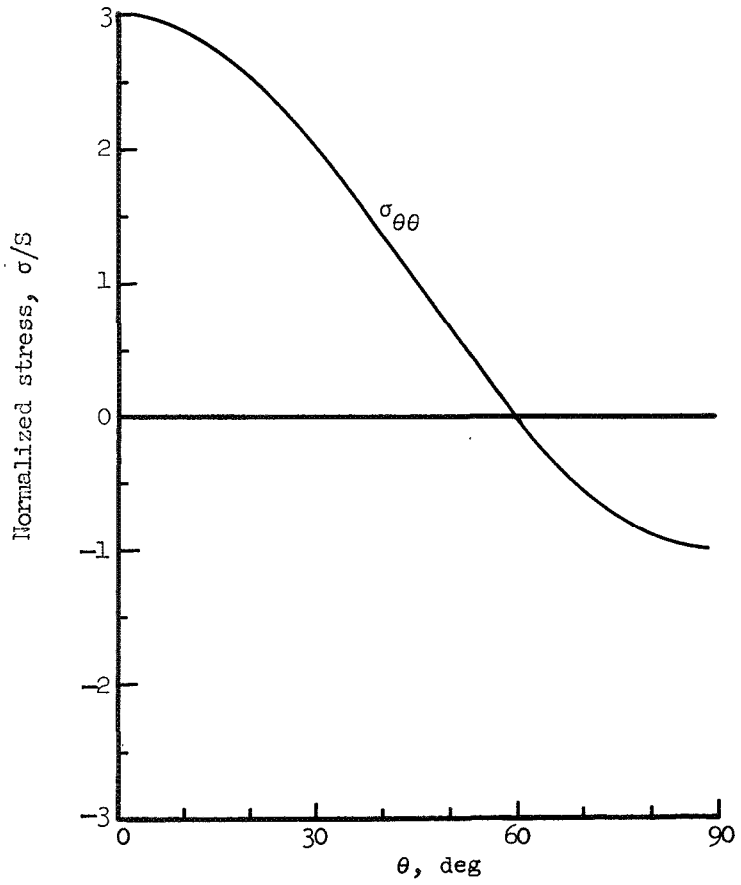

(a) Stress distribution along the hole boundary.

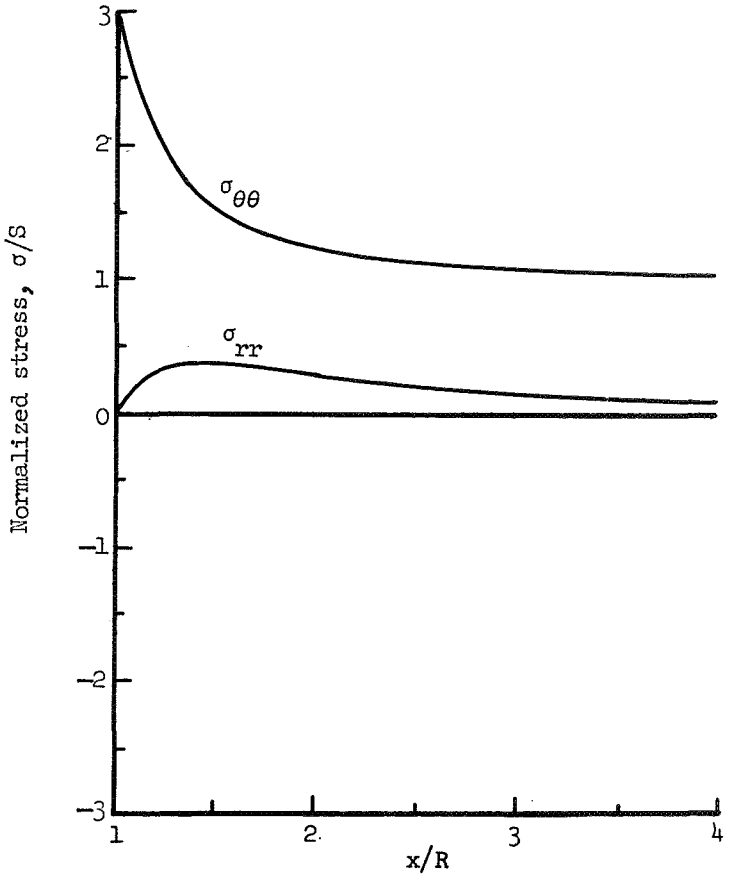

(b) Stress distribution on the transverse axis.

Figure 2.- Elastic stresses in a uniaxially loaded sheet with an open hole.

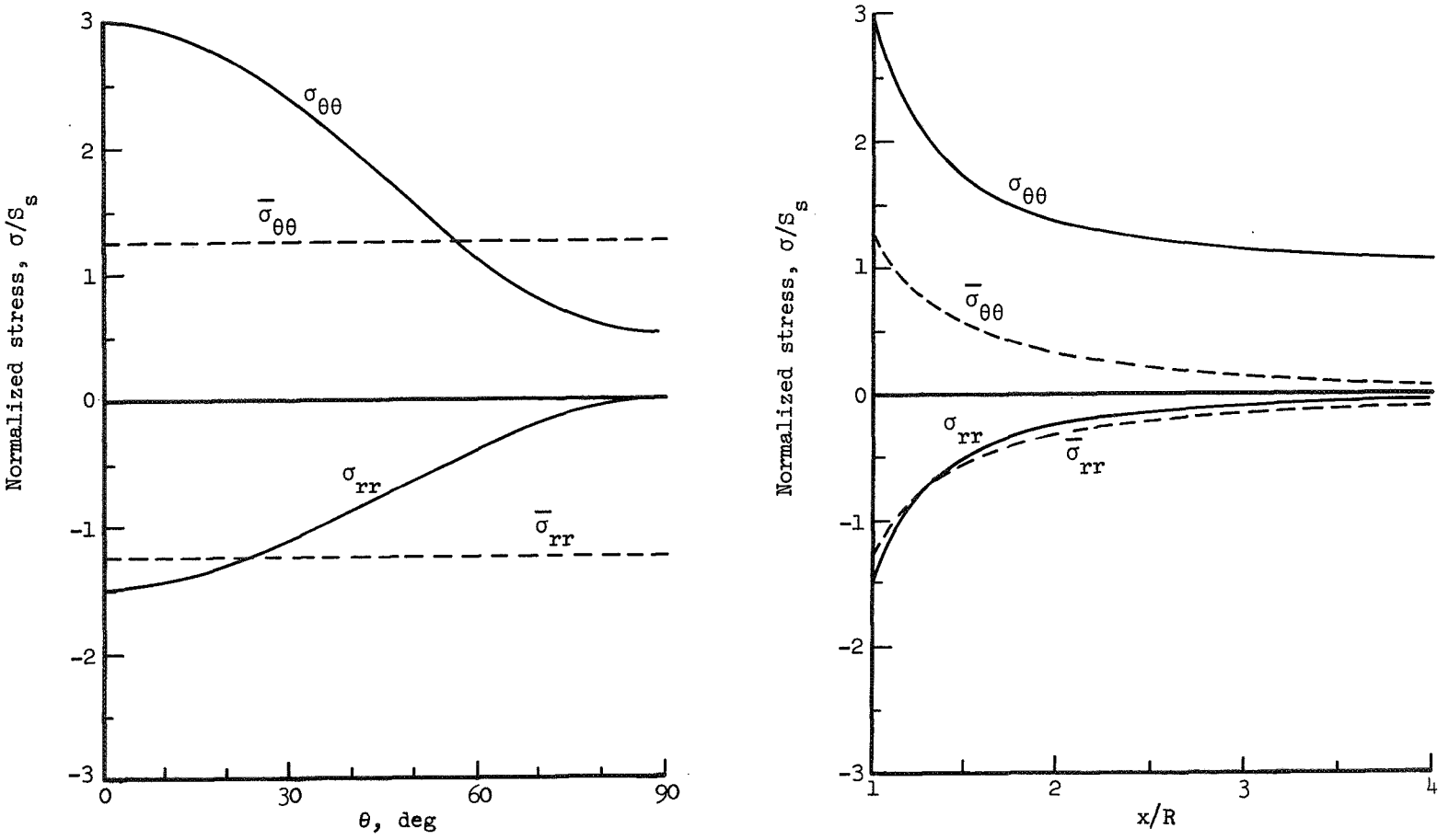

(a) Stress distribution along the hole boundary.

(b) Stress distribution on the transverse axis.

Figure 3.- Elastic stresses in a loaded sheet with a frictionless interference-fit bolt. $\frac{E_2}{E_1} = 1$; incipient separation.

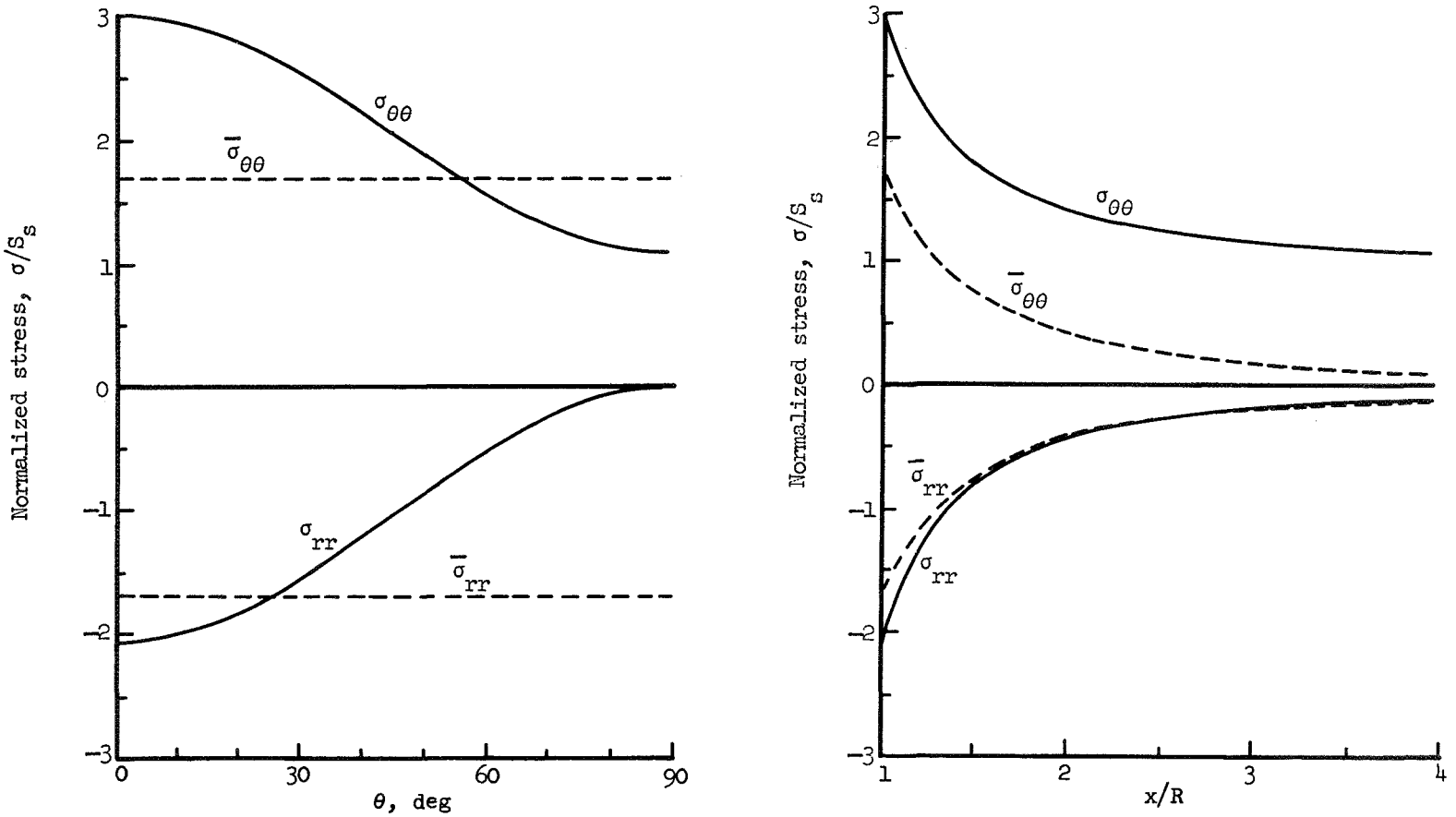

(a) Stress distribution along the hole boundary.

(b) Stress distribution on the transverse axis.

Figure 4.- Elastic stresses in a loaded sheet with a frictionless interference-fit bolt. $\frac{E_2}{E_1} = 3$; incipient separation.

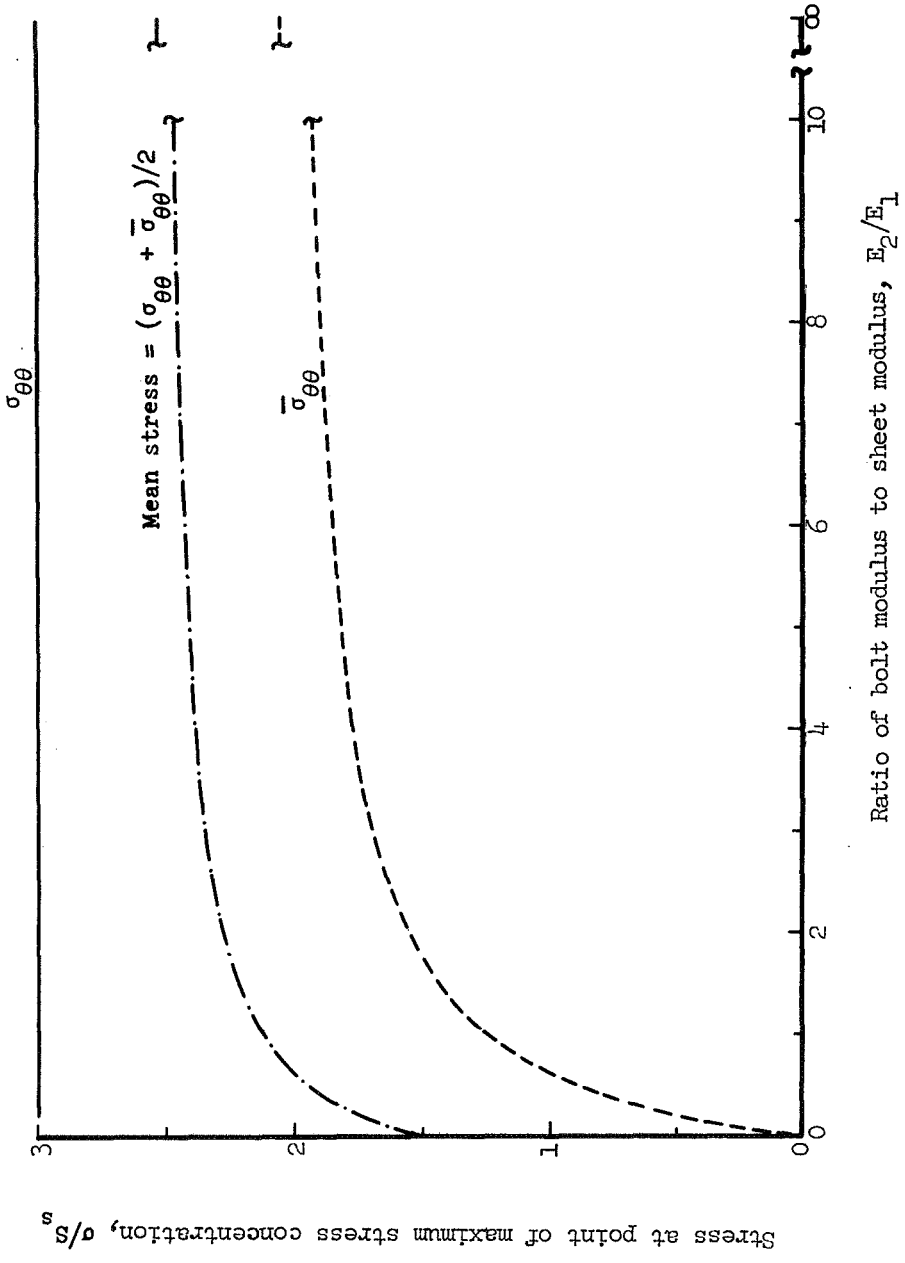

Figure 5.- Influence of E_2/E_1 on stress in a sheet with a frictionless-fit bolt. Incipient separation.

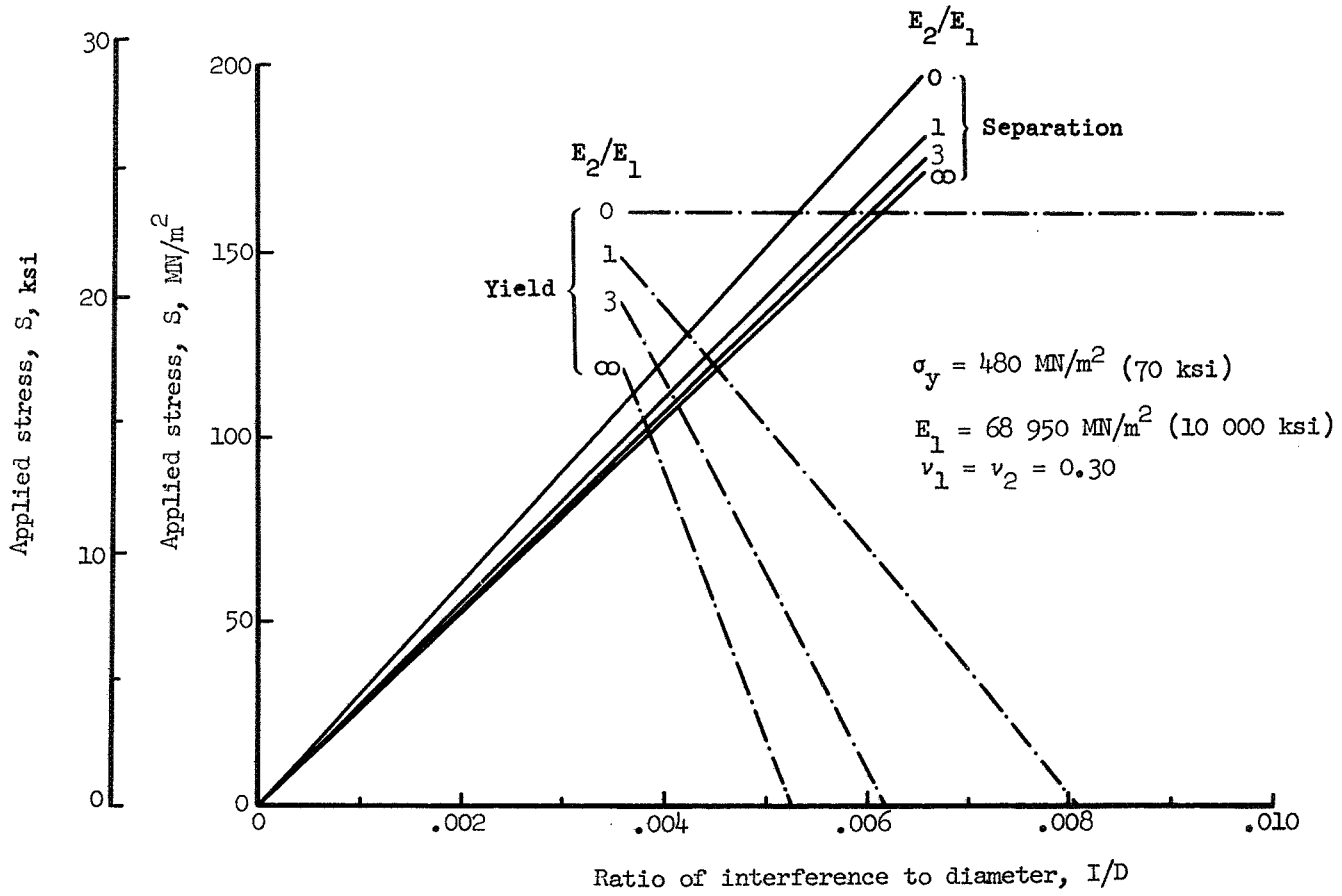

Figure 6.- Curves for onset of separation and sheet yielding for several ratios of bolt modulus to sheet modulus E_2/E_1. Frictionless fit.

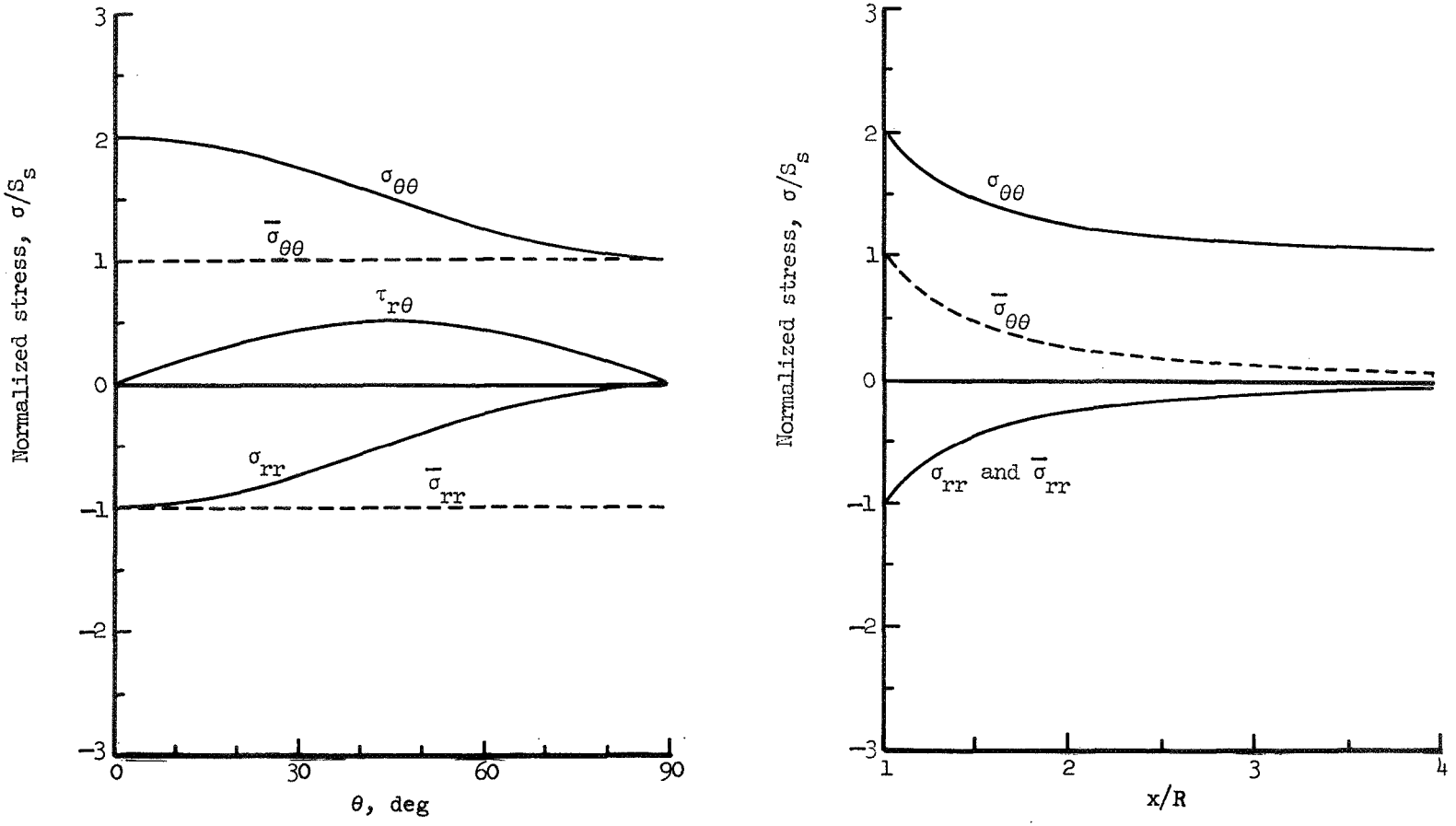

(a) Stress distribution along the hole boundary.

(b) Stress distribution on the transverse axis.

Figure 7.- Elastic stresses in a loaded sheet with a no-slip interference-fit bolt. $\frac{E_2}{E_1} = 1$; incipient separation.

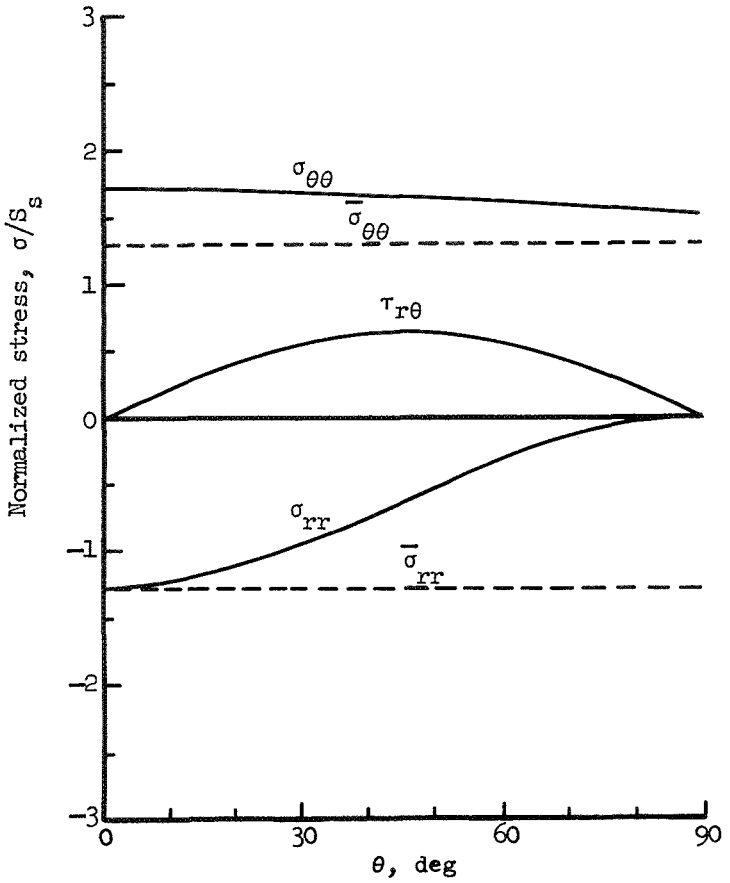

(a) Stress distribution along the hole boundary.

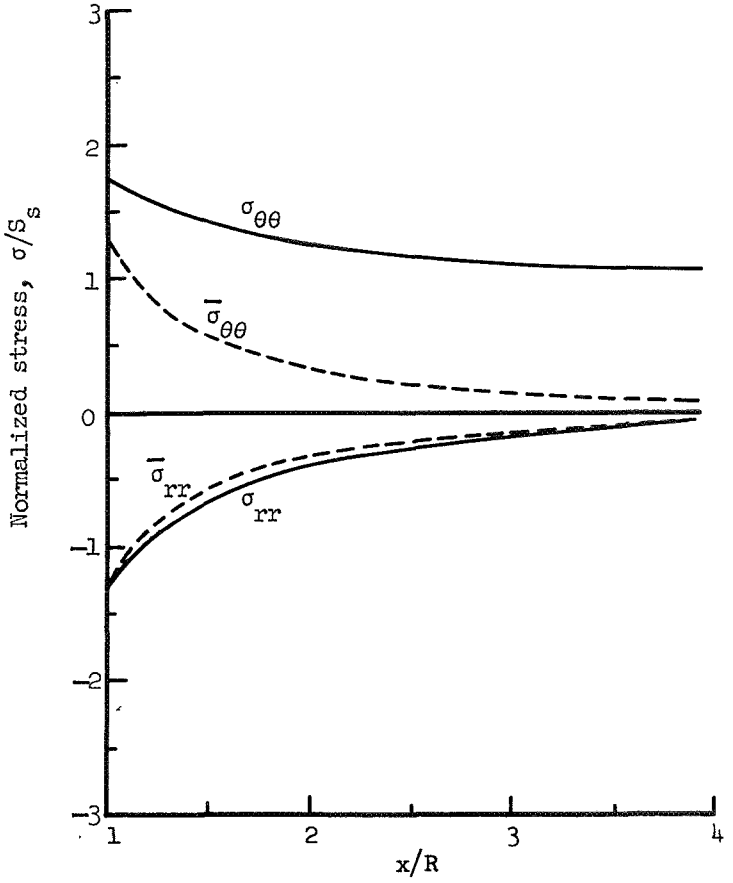

(b) Stress distribution on the transverse axis.

Figure 8.- Elastic stresses in a loaded sheet with a no-slip interference-fit bolt. $\frac{E_2}{E_1} = 3$; incipient separation.

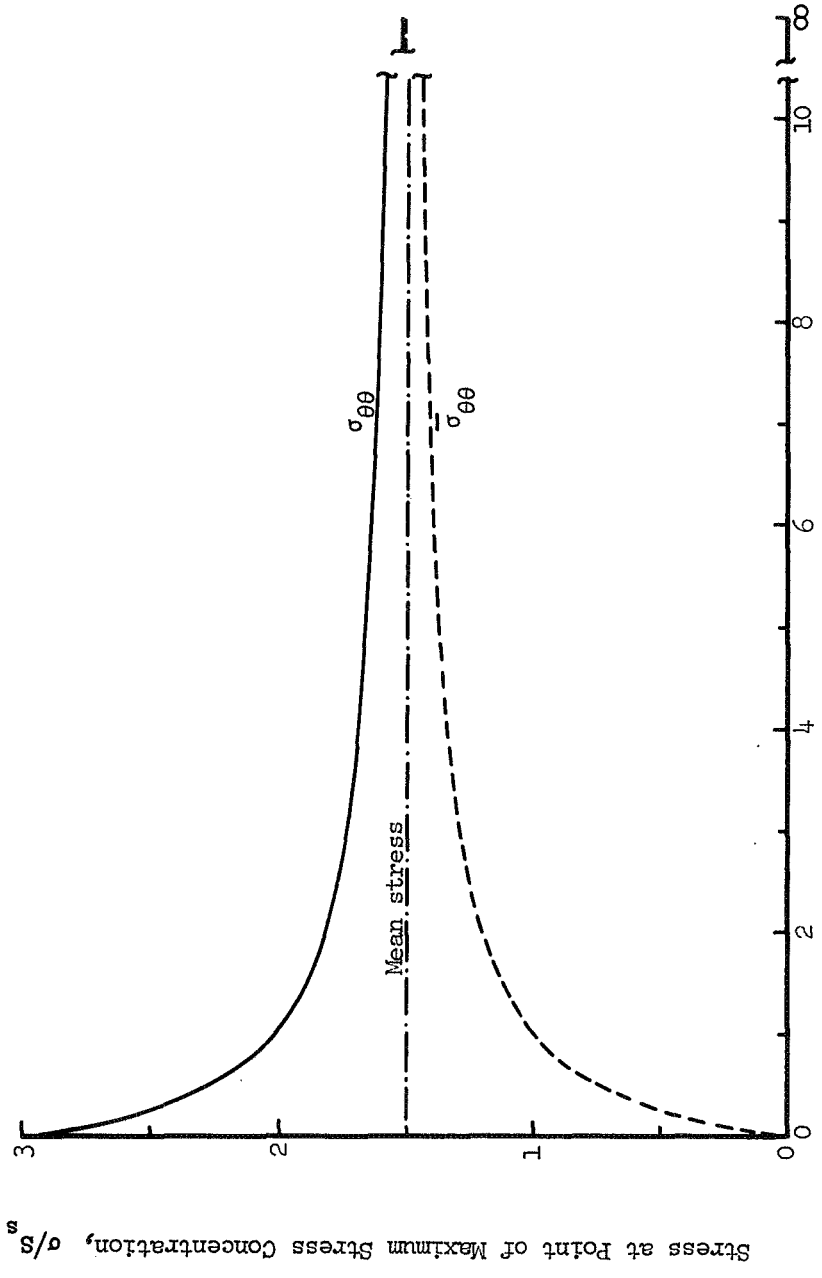

Figure 9.- Influence of E_2/E_1 on stress in a loaded sheet with a no-slip interference-fit bolt. Incipient separation.

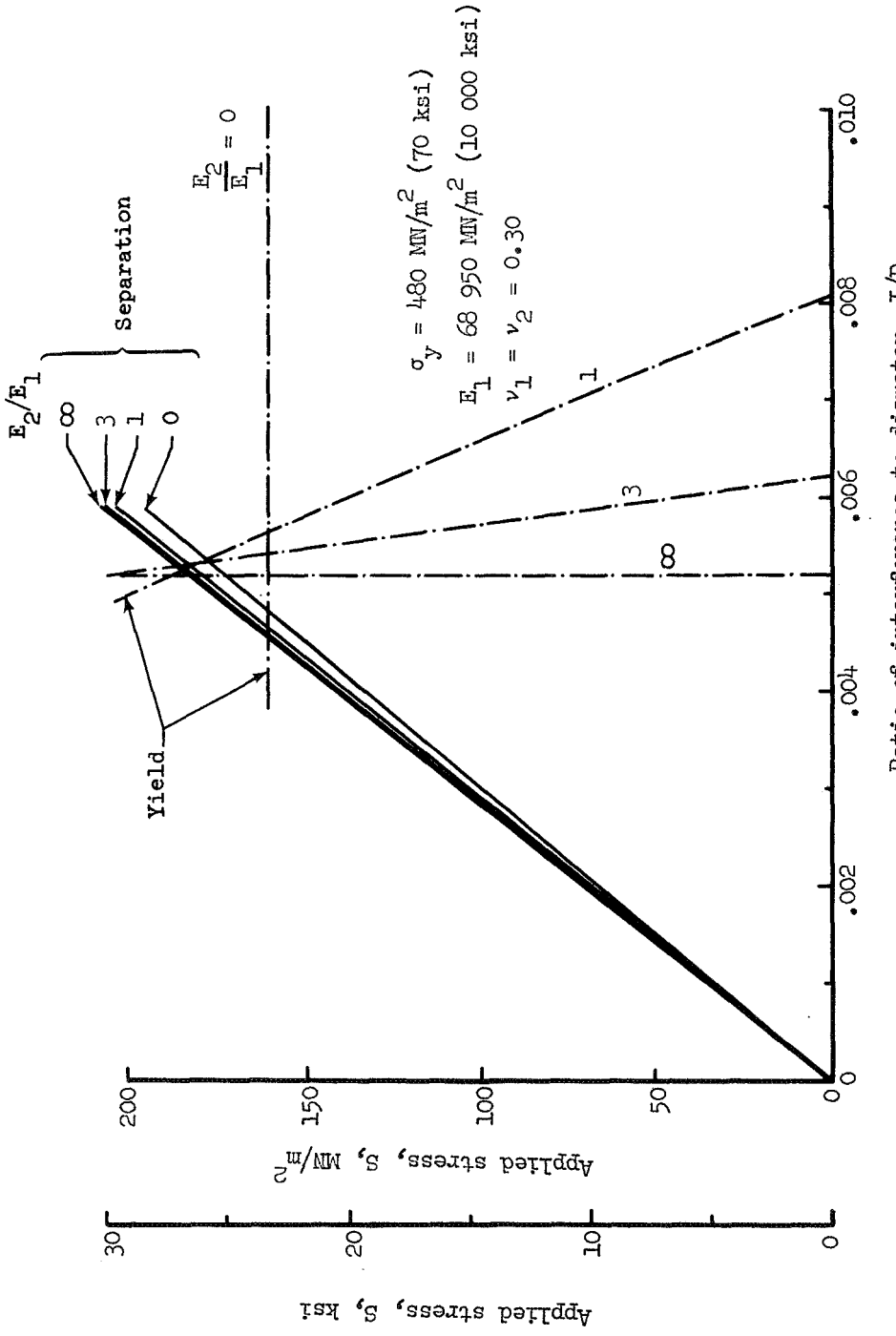

Figure 10.- Curves for onset of separation and sheet yielding for several ratios of bolt modulus to sheet modulus E_2/E_1. No-slip interference fit.

NATIONAL AERONAUTICS AND SPACE ADMINISTRATION
WASHINGTON, D.C. 20546

OFFICIAL BUSINESS
PENALTY FOR PRIVATE USE $300

SPECIAL FOURTH-CLASS RATE BOOK

POSTAGE AND FEES PAID
NATIONAL AERONAUTICS AND SPACE ADMINISTRATION
451

U.S.MAIL

POSTMASTER: If Undeliverable (Section 158 Postal Manual) Do Not Return

"The aeronautical and space activities of the United States shall be conducted so as to contribute . . . to the expansion of human knowledge of phenomena in the atmosphere and space. The Administration shall provide for the widest practicable and appropriate dissemination of information concerning its activities and the results thereof."

—NATIONAL AERONAUTICS AND SPACE ACT OF 1958

NASA SCIENTIFIC AND TECHNICAL PUBLICATIONS

TECHNICAL REPORTS: Scientific and technical information considered important, complete, and a lasting contribution to existing knowledge.

TECHNICAL NOTES: Information less broad in scope but nevertheless of importance as a contribution to existing knowledge.

TECHNICAL MEMORANDUMS: Information receiving limited distribution because of preliminary data, security classification, or other reasons. Also includes conference proceedings with either limited or unlimited distribution.

CONTRACTOR REPORTS: Scientific and technical information generated under a NASA contract or grant and considered an important contribution to existing knowledge.

TECHNICAL TRANSLATIONS: Information published in a foreign language considered to merit NASA distribution in English.

SPECIAL PUBLICATIONS: Information derived from or of value to NASA activities. Publications include final reports of major projects, monographs, data compilations, handbooks, sourcebooks, and special bibliographies.

TECHNOLOGY UTILIZATION PUBLICATIONS: Information on technology used by NASA that may be of particular interest in commercial and other non-aerospace applications. Publications include Tech Briefs, Technology Utilization Reports and Technology Surveys.

Details on the availability of these publications may be obtained from:

SCIENTIFIC AND TECHNICAL INFORMATION OFFICE

NATIONAL AERONAUTICS AND SPACE ADMINISTRATION

Washington, D.C. 20546